Electron-Electron Scattering at 500 Mev*

E. B. DALLY†
High-Energy Physics Laboratory, Stanford University, Stanford, California
(Received April 7, 1961)

The electron-electron differential scattering cross section has been measured with the use of a 500-Mev electron beam from the Stanford Mark III linear electron accelerator. Deviations were sought from the theoretical cross section as calculated in first-order perturbation theory (Møller scattering). The experimental results were compared with the Møller formula as corrected to the next order in perturbation theory by the work of Tsai.

Atomic electrons in a beryllium target foil constituted the target for the electron-electron scattering. The scattered electrons passed through a slit system which defined the angle of scattering and the solid angle. After the particles passed through the slit system, they entered a double-focusing magnetic spectrometer, which analyzed the scattered particles in momentum. The electrons emerging from the spectrometer were detected by a liquid Čerenkov counter. The incident beam was monitored with the use of a Faraday cup and an electronic current integrator.

In order to enhance the accuracy of the experiment, the experimental electron-electron scattering was compared to the elastic electron scattering from the target nuclei (Mott scattering).

The cross section was measured at approximately 2.6, 3.5, and 4.5 degrees in the laboratory system. These angles correspond to approximately 90, 107, and 120 deg in the center-of-mass system, respectively.

The theoretical magnitude of the radiative corrections is -5.5, -4.9, and -4.9% for the scattering angles 2.6, 3.5, and 4.5 deg, respectively. The average experimental deviation from the Møller formula found for the above angles was -3.0 $(\pm 2.3)\%$, -3.5 $(\pm 2.9)\%$, and -5.9 $(\pm 2.3)\%$, respectively, where the error cited is total statistical error. In addition to the statistical error there is a maximum estimated $\pm 2\%$ possible systematic error.

I. INTRODUCTION

A. Theoretical Background

THE fundamental interaction between elementary particles is one of the centers of interest in modern physics. The electron is one of the earliest known elementary particles, and the interaction between electrons (quantum electrodynamics) is supposed to be the best-founded branch of modern field theory. However, the experimental tests of the theory have been performed only at low momentum transfers (e.g., the Lamb shift), and the experiments which have been performed so far on the scattering of electrons by electrons have been done only below 16 Mev. It is known that the higher order effects (radiative corrections) manifest themselves mainly at high energies in scattering experiments, and it is important to be able to say that these corrections are well understood both theoretically and experimentally. This is the first experiment on the scattering of electrons by electrons to be performed at high energies.

When the Dirac equation is applied in the lowest order of perturbation theory to the calculation of the differential cross section for the scattering of electrons by electrons, the following expression is obtained for the laboratory system:

$$\frac{d\sigma}{d\Omega}(\theta)=2\left(\frac{e^2}{m_0v^2}\right)^2\frac{\gamma+1}{\gamma^2}\frac{(\gamma^*)^2\cos\theta}{[\cos^2\theta+(\gamma^*)^2\sin^2\theta]^2}\times\left\{\csc^4(\theta^*/2)-\csc^2(\theta^*/2)\sec^2(\theta^*/2)+\sec^4(\theta^*/2)+\left(\frac{(\gamma-1)^2}{\gamma}\right)[1+4\csc^2\theta^*]\right\}\text{ cm}^2/\text{sr}. \quad (1)$$

This is the well-known result first obtained by Møller.[1]

In the above expression θ is the angle of scattering in the laboratory system and θ^* is the corresponding angle in the center-of-mass system. The symbols e, m_0, and v are the electronic charge, rest mass, and incident velocity in the laboratory system, respectively. The quantity $\gamma=[1-v^2/c^2]^{-\frac{1}{2}}$ and $\gamma^*=[(\gamma+1)/2]^{\frac{1}{2}}$, which is the γ corresponding to the center-of-mass system. The terms which are dependent on the laboratory angle arise from the relation between the center-of-mass solid angle and the laboratory solid angle.

The terms in the result may be identified according to their physical origin. The first term in the curly brackets is the contribution from direct scattering; the third term is the exchange scattering part; while the second term is the interference term between direct and exchange scattering. The last term in the curly brackets is the part of the interaction which is contributed by the magnetic moment of the electron. The experiments which have been performed at low energies have verified the necessity of the presence of all these terms in the equation.

Until now, previous experiments on electron-electron scattering which have been performed with the use of particle accelerators have been done only at relatively low energies. Scott *et al.*[2] did an experiment similar to this experiment, with the use of an external betatron beam at 15.7 Mev. Barber *et al.*[3] performed a coincidence experiment at 6.1 Mev with the use of the Stanford Mark II linear electron accelerator. Kepes *et al.*[4] measured the cross section at 1–2.00 Mev with an electrostatic accelerator. The results of these experi-

* This work was supported in part by the joint program of the Office of Naval Research, the U. S. Atomic Energy Commission, and the Air Force Office of Scientific Research.

† Now at the Physics Institute, University of Zurich, Zurich, Switzerland.

[1] C. Møller, Ann. Physik **14**, 531 (1932).
[2] M. B. Scott, A. O. Hanson, and E. M. Lyman, Phys. Rev. **84**, 638 (1951).
[3] W. C. Barber, G. E. Becker, and E. L. Chu, Phys. Rev. **89**, 950 (1953).
[4] J. J. Kepes, B. Waldman, and W. C. Miller, Ann. Phys. **6**, 90 (1959).

ments were, in general, a few percent lower than the Møller cross section.

A positron-electron scattering experiment has been performed at 200 Mev with the use of a cloud chamber and the Stanford Mark III accelerator by Poirer *et al.*[5] Their result was a $(-13\pm9)\%$ deviation from the theoretical (Bhabha[6]) cross section. There have been no radiative corrections calculated for this experiment, so their result cannot at present be compared with such corrections.

B. Radiative Corrections

The radiative corrections for electron-electron scattering were first calculated by Redhead[7] and later by Polovin.[8] Both authors made two restrictions on their calculations. First, they restricted the energy k of the emitted photon to be $\ll mc^2$. Second, they limited $k_{\max}$ to an isotropic distribution in the laboratory system. These limitations are unrealistic for the present experiment. In this experiment, the maximum energy of the photon which is emitted can be as large as the energy of the undetected electron. Furthermore, the distribution is not isotropic, but tends to be peaked in the direction of the undetected electron. As a result of the restrictions, the results of Redhead and Polovin contain terms of the order $\alpha \ln^2(q^2/m^2)$, compared to one (q=four-momentum transfer in the scattering process, α is the fine structural constant). For this experiment these terms are as large as 30%. As the value of q is increased, the terms approach a relative value of 100%, which would make questionable the result of a perturbation calculation.

At the time of completion of this experiment, a calculation of the radiative corrections for this experiment was completed by Tsai.[9] Tsai calculated these corrections for two reasons. First, he wished to find out the origin of the existence of the $\alpha \ln^2(q^2/m^2)$ terms of Redhead and Polovin's results, and second, he wanted to develop the techniques which were necessary in order to calculate radiative corrections for systems in which the undetected particle can recoil with a large amount of energy which permits the undetected particle to radiate a high-energy photon. He showed that the results of Redhead and Polovin were correct within their restrictions. However, Tsai's result does not contain $\alpha \ln^2(q^2/m^2)$ terms. These terms canceled in his calculation.

The Tsai result predicts radiative corrections to the Møller cross section of approximately -5% for this experiment. The calculation has a maximum theoretical uncertainty of $\pm2\%$ which arises from the neglect of terms of the order of one compared to $\ln(q^2/m^2)$.

C. Breakdown of Quantum Electrodynamics

Because of the low momentum transfer in the center-of-mass system, this experiment is not sensitive to a possible breakdown of quantum electrodynamics of the types described in papers by Yennie *et al.*[10] and by Drell.[11] The center-of-mass four-momentum transfer varies approximately as $(2mE)^{\frac{1}{2}}$, where E is the incident laboratory energy. The experiments on electron-proton scattering which have been performed by Hofstadter[12,13] have already set limits on a possible breakdown of quantum electrodynamics below the distance probed in this experiment. For this experiment, with 500-Mev incident electrons, and for the case of 90° center-of-mass scattering angle, the momentum transfer expressed in fermis, is approximately 10 fermis. The distance probed in the electron-proton scattering experiments is about 0.8 fermi.

An experiment which is designed to test the limits of a possible breakdown of quantum electrodynamics is currently in preparation at Stanford. This is the colliding-beam experiment of O'Neill *et al.*[14]

D. Synopsis of This Experiment

The object of this experiment is to look for deviations from the Møller scattering cross section. Such deviations are expected because of radiative effects.

The procedure consisted of bombarding a beryllium target foil with a high-energy (500-Mev) electron beam from the Stanford Mark III linear electron accelerator. Electrons which scattered at a specified angle passed through an entrance slit which defined the solid angle and then entered a magnetic spectrometer which analyzed the electrons in momentum. After leaving the spectrometer, the electrons were detected by a liquid Čerenkov counter. The number of incident electrons was determined with the use of a Faraday cup and an electronic charge integrator. From this information a cross section could be determined. The cross section was actually obtained by comparing the electron-electron scattering to a known cross section: the Mott cross section[15] (relativistic elastic-nuclear scattering). The method of comparison was chosen in order to reduce the systematic errors of the experiment. This experiment has the advantages of good energy resolution and small or negligible corrections for plural scattering, energy straggling, and other target-thickness or geometric effects.

---

[5] J. A. Poirier, D. M. Bernstein, and Jerome Pine, Phys. Rev. **117**, 557 (1960).
[6] H. J. Bhabha, Proc. Roy. Soc. (London) **A154**, 195 (1936).
[7] M. L. G. Redhead, Proc. Roy. Soc. (London) **A220**, 219 (1953).
[8] R. V. Polovin, Soviet J. Phys. **4**, 385 (1956).
[9] Y. S. Tsai, Phys. Rev. **120**, 269 (1960); referred to as experiment II in this paper.
[10] D. R. Yennie, M. M. Lévy, and D. G. Ravenhall, Revs. Modern Phys. **29**, 144 (1957).
[11] S. D. Drell, Ann. Phys. **4**, 75 (1958).
[12] R. Hofstadter, Revs. Modern Phys. **28**, 214 (1956).
[13] R. Hofstadter, Ann. Revs. Nuclear Sci. **7**, 231 (1957).
[14] W. K. H. Panofsky, in *Proceedings of the 1960 Annual International Conference on High-Energy Physics at Rochester* (Interscience Publishers, Inc., New York, 1960), p. 769.
[15] N. F. Mott, Proc. Roy. Soc. (London) **A124**, 425 (1929).

Results are presented for the laboratory scattering angles of approximately 2.6, 3.5, and 4.5 deg. For an incident energy of 500 Mev, these angles correspond to 90, 107, and 120 deg in the center-of-mass scattering system, respectively. The results depend explicitly on the assumption of the validity of the Mott scattering formula at small angles, as corrected for radiative effects, and the validity of relativistic electron-electron kinematics.

II. APPARATUS

A. General

Electron-electron scattering presents experimental problems which require special consideration. Referring to Fig. 1, which is a plot of laboratory scattering angle vs center-of-mass scattering angle for 500-Mev incident electrons, one sees that the 90-deg center-of-mass angle becomes approximately 2.6 deg in the laboratory system. Thus, the angles of scattering in the laboratory are very small. The relationship connecting center-of-mass angle θ^* and the laboratory angle θ is

$$\cos\theta^* = \frac{2-(\gamma+3)\sin^2\theta}{2+(\gamma-1)\sin^2\theta}. \tag{2}$$

Of additional interest is the relationship between the energy in the laboratory system of the scattered electron as a function of laboratory angle. The relation is

$$E' = m\frac{[(E+m)+(E-m)\cos^2\theta]}{[(E+m)-(E-m)\cos^2\theta]}. \tag{3}$$

Here E' is the scattered energy and E is the incident energy. Figure 2 is a plot of this function for $E=500$ Mev. The scattered energy varies extremely rapidly as a function of angle. At 2.6 deg, the scattered energy changes at a rate of approximately 100 Mev/deg.

It was desired to use a spectrometer to analyze the scattered particles in energy. From the above considerations, one can see that such a spectrometer must be able to collect scattered electrons at small angles, and it must not interfere with the incident electron beam.

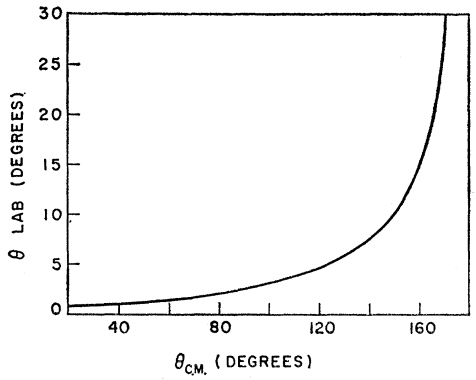

FIG. 1. Electron-electron scattering. Laboratory scattering angle vs center-of-mass scattering angle. E (incident) = 500 Mev.

B. Accelerator

The Stanford Mark III accelerator has been described elsewhere.[16] After acceleration, the particles enter a beam translation area consisting of two magnets.[17] This system is shown schematically in Fig. 3. In this system, the beam is analyzed in energy, and the spread of beam energy is defined. The beam can be steered and also focused through the use of the rotating pole tips.

C. Spectrometer

The constructed spectrometer has a C-type cross section. It is a double-focusing spectrometer constructed according to the theory contained in the article by Judd.[18] The bending radius of the central orbit is 36 in., and the angle of deflection is 90 deg. The target to magnet distance which was selected is 65 in., which gives a distance of 107 in. from magnet to focal plane.

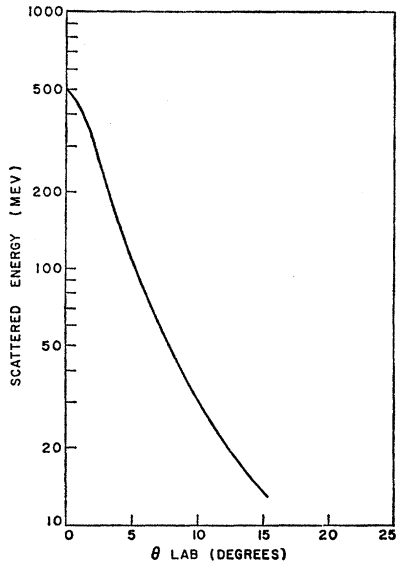

FIG. 2. Electron-electron scattering. Scattered electron energy vs laboratory angle. E (incident) = 500 Mev.

The magnetic field shape parameter n has a value of $\frac{1}{2}$ for a double-focusing spectrometer. The n value was carefully measured for several magnetizing currents in the range which was used in the experiment. The measurements showed a 1–2-in. region where the n value is within $\frac{1}{2}\%$ of the desired value of $\frac{1}{2}$. From these measurements, one could with confidence select entrance-slit sizes for different scattered energies which kept the electron orbits in the region where n equaled $\frac{1}{2}$. The measurements of n were performed with the use of the same rotating coil device which was used as a field monitor during data collection and the n values measured had less than 1% error.

[16] M. Chodorow, E. L. Ginzton, W. W. Hansen, and Staff, Rev. Sci. Instr. **26**, 134 (1955).
[17] K. L. Brown, Rev. Sci. Instr. **27**, 959 (1956).
[18] D. L. Judd, Rev. Sci. Instr. **21**, 213 (1950).

The energy calibration of the spectrometer was accomplished through the use of the accelerator beam. The accelerator beam had been calibrated by a floating-wire calibration[19] on the deflecting magnet of the beam translation system. This calibration has an estimated error of $\pm\frac{1}{2}\%$. The magnetic field of the deflecting magnet was adjusted and monitored for a data run by the use of a proton-resonance probe. The energy calibration of the deflecting magnet was expressed in terms of the frequency of the proton resonance. The energy of the accelerator was then easily reproducible to 1 part per 10 000 from run to run. The spectrometer calibration was made by passing the accelerator beam through the spectrometer and measuring the field value which caused the incident beam to be focused at the central-orbit position of the focal plane.

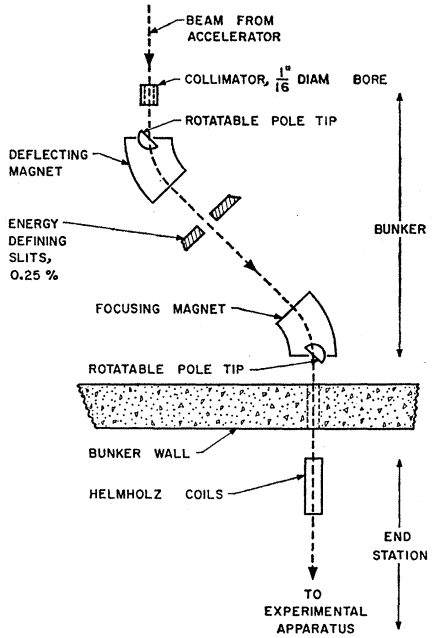

FIG. 3. Beam translation system.

D. Vacuum System

A vacuum chamber was constructed for the spectrometer. The vacuum chamber included target chamber, a connecting arm to the spectrometer, a spectrometer vacuum chamber and a vacuum pipe from spectrometer to detector. After the electron beam went through the target it passed out of the vacuum chamber through a thin Mylar window which formed one side of the connecting arm from the target chamber to the spectrometer. The window was sealed with Neoprene cord and a clamping frame.

The target chamber contained a movable target holder in the form of a ladder. This was remotely controlled from the counting room. During a run a zinc sulfide fluorescent screen which had been placed in one of the target spaces was inserted into the beam to a predetermined point, and the shape, size, and position of the beam spot were viewed with the use of a closed-circuit television system.

[19] E. A. Allton (private communication).

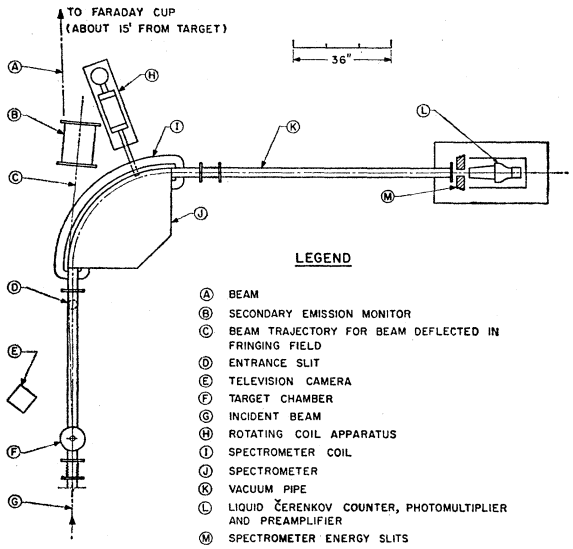

FIG. 4. Experimental arrangement.

E. Auxiliary Equipment

The target chamber was connected directly to the accelerator drift tube by a flexible connection which permitted scattering to angles as large as 10 deg.

An entrance slit system was included in the vacuum connecting arm. The slit was made of lead, and the final hole size was obtained by pressing a die through the lead. The die was measured to give the entrance slit size.

The particle detector was located in a counter house constructed of 8-in. steel walls. The entire apparatus was mounted on a small carriage which traveled on tracks on the 36-in.-spectrometer gun mount. A schematic layout of the apparatus is shown in Fig. 4.

F. Particle Detection

The detection system consisted of a liquid Čerenkov counter which was attached to a 5-in. photomultiplier. The Čerenkov counter was made in the shape of a truncated cone about 12 in. long. The fluid which was used was Fluorochemical-75.

G. Rotating-Coil Apparatus

A piece of apparatus which was important for this experiment was a rotating-coil device[20] that was constructed to monitor the spectrometer magnetic field.

[20] F. Bumiller, J. Oeser, and E. Dally, *Proceedings of the International Conference on Instrumentation for High-Energy Physics, Berkeley, 1960* (to be published).

The rotating-coil system was sensitive to field changes of 1 part per 10 000 and was reproducible from day to day to better than 5 parts per 10 000. These properties were checked in a test magnet which was monitored by a proton-resonance probe.

H. Beam Monitoring

The accelerator beam was monitored with the use of a Faraday cup or secondary emission monitor (SEM).[21,22] The signal from either of these devices was integrated with the use of a vibrating reed electrometer. Recent checks of the Faraday cup[22] indicate the efficiency to be 100% in the energy range 60–600 Mev. No deviation from a response of 100% could be detected, but the limit of sensitivity of the tests was about $\pm 1\%$.

I. Angular Alignment

At the very small angles of scattering in the laboratory at which the cross section was measured, a small absolute error in the knowledge of the angle of scattering would produce a large percentage error in the measured cross section. Hence, it was extremely important that the angle of scattering be accurately known.

One can predict the position of the beam line for the accelerator from the alignment of the beam translation system, but this alignment procedure does not assure one that the beam which emerges from the beam translation system actually follows the predetermined line. The beam might cross this line at a small angle. The apparatus was aligned for an experiment with reference to the beam line which was determined from the alignment of the beam translation system.

The angle which the beam makes with the surveyed beam line was measured and found to be approximately 0.02 ($\pm 20\%$) deg. This angle fluctuated between 0.010 and 0.030 deg from data run to data run and changed slightly with accelerator energy during the same data run.

When the measured angle and the value of the incident beam energy were inserted into Eq. (3), the predicted value of the scattered energy was in complete agreement with the scattered energy measured by the spectrometer within the error of the energy calibration of the spectrometer and the angular uncertainty. Because the angular deviation of the beam varied slightly from run to run, the angle of scattering was determined by using the knowledge of the incident and scattered energy of the electron-electron peaks. The scattered energy from electron-electron scattering is very sensitive to small angular changes. Hence, the angle of scattering was determined to within the accuracy of the accelerator energy calibration.

J. Target Material

The choice of the target material was based on three considerations. First, a low-Z material was desired to assure the validity of the Mott cross section. Second, a low-Z material was desired in order to keep the contribution to the scattering from the bremsstrahlung process as small as possible, since this contribution increases as Z^2 and the electron-electron scattering cross section increases only as Z. Third, because the experiment was so sensitive to multiple scattering effects, a material with a long radiation length was required. The lowest-Z material available in thin foil form is beryllium ($Z=4$, radiation length $\simeq 69$ g/cm^2). The target foil was machined, and hence somewhat nonuniform in thickness. The effect of this uncertainty is assumed to cancel because of the experimental method employed. The target was approximately $2\frac{1}{2}$ mils in thickness, and was measured to be 10.0 ($\pm 4\%$) mg/cm^2.

III. EXPERIMENTAL PROCEDURE

A. Experimental Method

In this section we outline the procedure followed in the performance of the experiment and some important details are discussed.

The measurement of the electron-electron cross section was accomplished through the comparison of the experimental electron-electron scattering cross section with the experimental results obtained from the elastic-nuclear scattering data from the same target. For this experiment, at the very small angles of scattering, the elastic-nuclear scattering is essentially Mott scattering. The largest correction to the Mott formula is from the radiative effects,[23,24] which amounted to a 10% correction. The combined effects of form factor, nuclear recoil and second Born approximation[25] contribute a -0.7% correction to the Mott cross section for the conditions of this experiment.

The outline of the procedure used to measure the cross section is as follows: (a) electron-electron scattering peaks were obtained at the angles of 2.6, 3.5, and 4.5 deg in the lab; (b) an elastic-nuclear scattering peak was taken at 4.5 deg with an incident beam energy which corresponded to the scattered energy of the electron-electron peak taken at 4.5-deg scattering angle. At small scattering angles the incident and scattered energy are the same for nuclear scattering; (c) a ratio was formed of the areas of the electron-electron peak to the area of the elastic-nuclear scattering peak. This ratio is multiplied by appropriate factors to take into account the difference in the number of electrons passing through the target. The ratio should be equal to the theoretical ratio of the cross sections; (d) to

[21] G. W. Tautfest and H. R. Fechter, Rev. Sci. Instr. **26**, 229 (1954).
[22] F. Bumiller and E. Dally, in *Proceedings of the International Conference on Instrumentation for High-Energy Physics, Berkeley, 1960* (to be published).
[23] J. Schwinger, Phys. Rev. **75**, 898 (1949).
[24] H. Suura, Phys. Rev. **99**, 1020 (1955).
[25] W. A. McKinley and H. Feshbach, Phys. Rev. **74**, 1759 (1948).

obtain the electron-electron cross section, the ratio is multiplied by the corrected Mott formula as evaluated for the proper incident energy and scattering angle.

By the use of the comparison method, uncertainties arising from target thickness and target density were canceled.

The method of reducing the incident energy of the beam to give a final energy for elastic-nuclear scattering close to the final energy of electron-electron scattering reduces or eliminates uncertainties which arise from spectrometer transmission efficiency, spectrometer dispersion, and detection efficiency, since electrons of nearly the same energy entered the spectrometer for either electron-electron or elastic-nuclear scattering.

B. General Considerations

For this experiment, there are several important matters which are now considered. (i) Because the scattering angles are small, and the elastic-nuclear cross section varies approximately as $1/\theta^4$, a small error in the determination of the scattering angle would give a large error in the value of the normalizing cross section. (ii) The extremely rapid variation of the scattered energy as a function of scattering angle for electron-electron scattering requires the incident beam to be very stable in position. (iii) The rapid dependence of scattered energy upon the scattering angle in electron-electron scattering means that there is no compensation by "scattering-out" for electron-electron scattering. This is because each scattered ray which comes from the target at a different angle has a different energy. The ray might still enter the spectrometer through the entrance slit; however, the spectrometer is adjusted to accept only a very narrow energy range which corresponds to scattering at a well-defined angle. Therefore, for electron-electron scattering, the multiple scattering losses are large. (iv) On the other hand, for elastic-nuclear scattering, there is a negligible dependence of scattered energy on the angle of scattering at the small angles. This fact results in the approximate cancellation of the scattering-in and scattering-out at the entrance slit for elastic-nuclear scattering. The amount of cancellation depends on the size of the entrance slit, the properties of the target material, and the curvature of the cross section as a function of angle.

C. Appearance of the Electron-Electron Peaks

With some of the above considerations in mind, we now discuss the shape of the scattering peak obtained from electron-electron scattering. The shape of an experimental peak from Møller scattering, with no radiative corrections, for a point beam spot, no multiple scattering and perfect resolution (referred to as the ideal case), would appear approximately as indicated in Fig. 5 for the case of 500-Mev incident electrons scattered at about 2.6 deg. The curve labeled "Møller cross section" is normalized to one at the 250-Mev point.

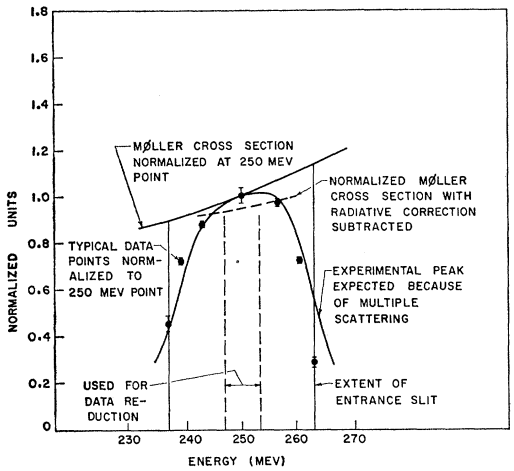

FIG. 5. Ideal vs estimated electron-electron scattering peak for E (incident) = 500 Mev and $\theta_{lab} \simeq 2.6$ deg.

The ideal peak is the Møller cross section curve bounded by the two vertical lines labeled "extent of entrance slit." That is, because of the strong dependence of scattered energy on the angle of scattering, each ray which is scattered at a different angle enters the entrance slit with a different energy. The entrance slit would define very sharply the sides of the peak. However, because there is multiple scattering and because the beam spot does have a finite size, from consideration of (iii) one can see that the peak is modified approximately as shown by the smooth curve in Fig. 5. This curve was obtained by the calculation of the effects of a finite source size and the effects of multiple scattering upon the ideal curve. One can understand that the scattered ray, which would pass just inside the slit edge, loses half its intensity when it is spread because of multiple scattering. Data points taken from an experimental peak and normalized to unity at the 250-Mev point, are shown for a comparison with the estimated peak. This procedure illustrates the origin of the peak shape. Because the peaks are rather wide ($\sim$25 Mev), the effects of spectrometer dispersion and energy spread of the incident beam are small and do not visibly affect the shape or the width of the electron-electron peaks.

Small movements of the beam position on the target strongly affect the data points which are located at the sides of the electron-electron peaks. The central part of the electron-electron peaks is relatively unaffected by small beam fluctuations and multiple-scattering losses if the entrance slit is made sufficiently wide.

The dashed line in Fig. 5 is the result of applying the radiative corrections, which were calculated by Tsai, to the normalized cross section. Note that the corrections not only shift the Møller cross section, but that the slope is also changed.

D. Collection of the Data

In the collection of data, a preparatory procedure was carefully followed for each data run. On each data run considerable time and care were expended to focus and to shape the beam spot, and to make the conditions from data run to data run as nearly the same as possible.

The SEM was calibrated by comparison of its response with the Faraday cup. The SEM efficiency was 22–25%, depending upon the incident energy.[22] After calibration, the SEM had to be positioned properly before data could be taken. Referring to Fig. 4, the trajectory of the beam is curved after leaving the vacuum chamber because of the influence of the fringing field of the spectrometer. This bending of the beam, which varied depending upon the angle of scattering, the incident energy, and the spectrometer current, caused the beam to miss the Faraday cup. Therefore, a portable monitor such as the SEM had to be used for some data points. The SEM was located properly by viewing the beam spot position on zinc sulfide screens placed over the entrance and exit windows of the SEM. The spot position was observed by a telescope-and-mirror arrangement on the exit screen and by a closed-circuit television system on the entrance screen. The SEM was alternately observed and positioned until the beam spot was located on the center line of the SEM.

In order to collect the data, the spectrometer current was set well above the peak position and data points were recorded for a fixed number of incident electrons as measured by the charge integrator. The spectrometer current was lowered in small steps and data was taken at each setting. Successive points were recorded until a peak was traced out. The beam spot position was checked between points on the peak. Typical electron-electron data peaks taken at 2.6, 3.5, and 4.5 deg are shown in Figs. 6, 7, and 8, respectively. The error bars which are shown are the standard deviation of the number of counts which was recorded. The plotted points have been corrected for counting rate losses. The points which are indicated as background points arise from electrons which scattered from the exit window of the vacuum chamber. These points were taken with the target out of the beam. A continuous line of points above the background is found at energies above and below the electron-electron peak (but are not shown in the figures). These points come from the electrons which have undergone a bremsstrahlung process.

The elastic-nuclear scattering peaks were taken in a manner similar to the electron scattering peaks. A typical peak, taken at 4.5 deg is shown in Fig. 9.

IV. REDUCTION OF THE DATA

A. Method

The general approach of the method of data reduction has been given above. In principle, one uses the area under the scattering peaks to obtain the cross section. However, in view of the discussion concerning the multiple-scattering losses on the electron-electron peaks, one can see that the area under the experimental peaks would give a cross section which is much smaller than the actual cross section. The true area could be obtained (in principle) by calculation of the multiple scattering losses. The corrections for these losses would be large, and a small error in making these corrections could make an error in the final result which is as large as the radiative corrections. One uncertainty in the corrections is the slope of the cross section curve vs angle of scattering. The radiative corrections indicate that the slope is different from the slope of the Møller cross section. Another uncertainty arises from the large fluctuations of the data points on the sides of the peaks which are caused by small drifts of the beam position.

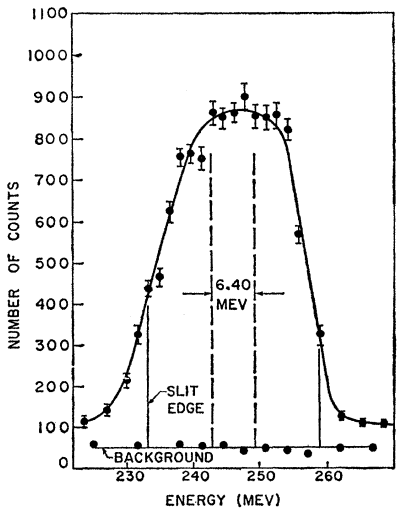

FIG. 6. Electron-electron peak—2.6°. E (incident) = 500 Mev.

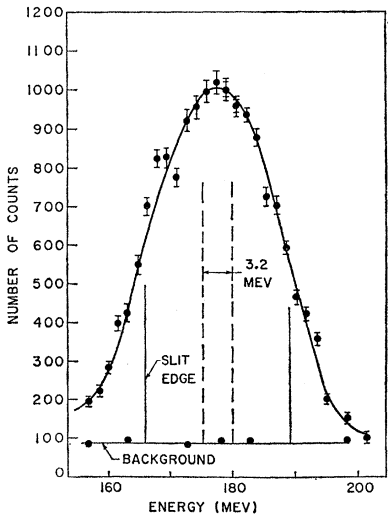

FIG. 7. Electron-electron peak—3½°.

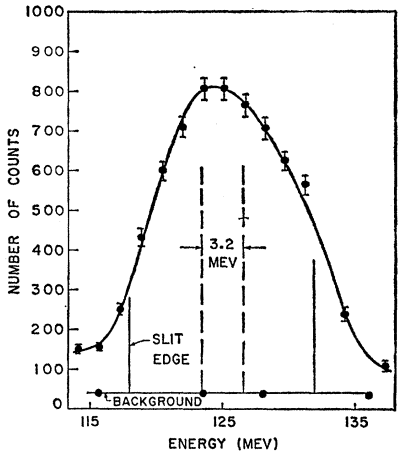

FIG. 8. Electron-electron peak—$4\frac{1}{2}°$.

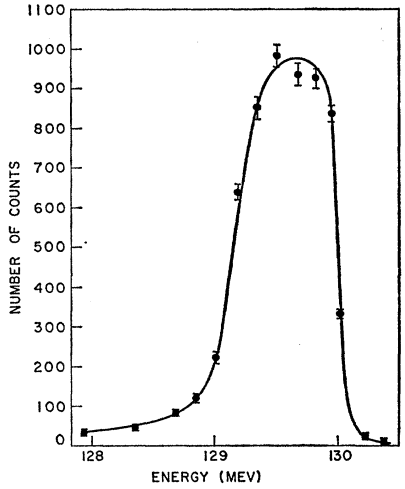

FIG. 9. Elastic-nuclear scattering peak for beryllium—$4\frac{1}{2}°$. E (incident) = 129.5 Mev.

The central part of the electron-electron peaks is relatively unaffected by beam spot size, multiple scattering, and small beam drifts. For these reasons, only the central part of the electron-electron peaks was used for data reduction. The region of the peak which was used is indicated on the peaks shown in Figs. 6–8. The width of the region, expressed in energy units, defines the angular interval of scattering through the relationship between scattered energy and angle of scattering. The solid angle is proportional to the product of the angle subtended by the vertical dimension of the entrance slit and the angular interval derived from the width of the region taken from the data peak. The interval used corresponded to about $\frac{1}{4}$ the actual width of the entrance slit. In the reduction of the data, the ratio of the solid angles of the electron-electron data to the elastic-nuclear data becomes the ratio of the angular width of the region from the electron-electron peak to the angular width of the entrance slit. The vertical dimension cancels in this ratio. It is possible to use this procedure because the energy calibration of the accelerator and the spectrometer were well known, and the slope of the spectrometer energy calibration was well established and linear.

B. Corrections

The area used to calculate the cross section from the electron-electron peaks was the area of the region above the background. This area contained electrons which were contributed by all other processes in addition to electron-electron scattering. Consideration shows that the only process which contributed significantly was the one in which electrons had undergone a bremsstrahlung process. The magnitude of this effect was calculated from the results of Berg and Lindner.[26] The effect amounted to a $3\frac{1}{2}$, $2\frac{1}{2}$, and 1% contribution at the scattering angles 2.6, 3.5, and 4.5 deg, respectively. A comparison of these calculations with the experimental scattering found in the continuum at the high-energy end of the electron-electron peaks gives excellent agreement.

The measured areas of the elastic-nuclear scattering peaks were corrected for radiative effects. This correction was approximately 10%.

The multiple-scattering and beam-spot-size effects contributed a 1%, $\frac{1}{2}$%, and negligible correction to the electron-electron peaks at 2.6, 3.5, and 4.5 deg, respectively. The elastic-nuclear scattering peak at 4.5 deg required less than a 1% multiple scattering correction. An additional correction factor of $\frac{1}{2}$% was included in the elastic-nuclear peaks because of the finite solid angle subtended by the slit. The multiple-scattering and beam-spot-size corrections were made numerically by a folding of the two effects. The multiple-scattering calculations used were those of Molière[27] as presented in the work of Hanson, *et al.*[28] These results have been shown by Mozley *et al.*[29] to be valid at high energies.

Other corrections arising from target thickness and geometric effects were negligible. Atomic binding, screening, and plural-scattering effects were also negligible.

C. Assignment of Errors

The total statistical counting error for each data point of the electron-electron and elastic-nuclear peaks is about 2% or less. This error includes the error which is propagated by the subtraction of the background. The error assigned to the ratio of electron-electron to elastic-nuclear areas is the square root of the sum of the

[26] R. A. Berg and C. N. Lindner, Phys. Rev. **112**, 2072 (1958).

[27] G. Molière, Z. Naturforsch **3a**, 78 (1948).

[28] A. O. Hanson, L. H. Lanzl, E. M. Lyman, and M. B. Scott, Phys. Rev. **84**, 634 (1951).

[29] R. F. Mozley, R. C. Smith, and R. E. Taylor, Phys. Rev. **111**, 647 (1958).

TABLE I. Summary of the results.

Angle[a] (degrees) (lab)	Center-of-mass angle (degrees)	Experimental cross section (10^{-25} cm^2/sr)	Møller cross section (10^{-25} cm^2/sr)	% difference between Møller and experimental cross sections	Calculated radiative corrections (percent)
4.46	120	0.902(±0.037)	0.944	−5.2(±4.1%)	−4.9
4.48+	120	0.893(0.039)	0.940	−5.0(±4.1%)	−4.9
3.49+	107	1.10 (0.046)	1.14	−3.5(±4.1%)	−4.9
3.51+	107	1.09 (0.045)	1.13	−3.5(±4.1%)	−4.9
2.61+	90	1.78 (0.074)	1.77	+0.6(±4.1%)	−5.5
2.63+	90	1.71 (0.071)	1.75	−2.3(±4.1%)	−5.5
2.63*	90	1.62 (0.067)	1.75	−7.4(±4.1%)	−5.5
4.56*	120	0.865(0.036)	0.935	−7.6(±4.1%)	−4.9

[a] In the table + and * indicate data normalized to the same 4½-deg elastic-nuclear scattering peak.

squares of the statistical errors of each peak. The result is a 3% error for the ratio of areas for each point.

The total systematic error contributed by the uncertainty of the solid angle, integration errors, and uncertainty of SEM efficiency is estimated to be less than 2%.

The principle error is a 2.8% error in the evaluation of the theoretical Mott cross section because of the uncertainty of the exact value of the scattering angle. The error in this angle varied from run to run in a random fashion, so that this error is included as a random error and folded into the 3% counting error for each point. The total statistical error becomes 4.1% for each measured point.

No error is included for a possible change of Faraday cup efficiency in the energy range 125–500 Mev. Furthermore, no error is included for a possible change of spectrometer transmission efficiency or particle detection efficiency in the range 125–250 Mev. The Mott cross section is assumed to be theoretically correct, and no error is assigned to it.

E. Results

The results are given in Table I. The experimental and Møller cross sections are given in columns 3 and 4, respectively. The percentage difference of the experimental results from the Møller cross section is given in column 5. The last column contains the radiative corrections as calculated by Tsai.

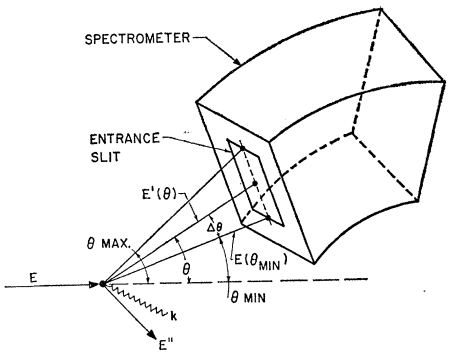

FIG. 10. Experimental geometry for radiative corrections.

V. COMPARISON WITH THEORY

A. Theory

The expression for the radiative correction to the Møller formula is

$$d\sigma/d\Omega = (d\sigma/d\Omega)(\text{Møller})[1+\delta(\theta)], \tag{4}$$

where $\delta(\theta)$ is the radiative correction calculated by Tsai. It is given in a special form for angles ≥ 90 deg center-of-mass scattering as

$$\delta(\theta)=\frac{-4\alpha}{\pi}\left\{\frac{23}{18}-\frac{11}{12}\ln\left(\frac{2E'}{m}\right)+\ln K\left[\ln\frac{2E'(E-E')}{mE}-1\right]-\tfrac{1}{4}\ln K\left[\ln\frac{E}{m}-1\right]+\tfrac{1}{4}\ln\frac{E}{m}\right\}, \tag{5}$$

where

$$K=\frac{\theta}{2\Delta\theta}\left[\frac{E\times E'}{(E-E')^2}\right]^{\frac{1}{3}}.$$

The significance of the symbols used is shown in Fig. 10 for an experimental arrangement. They are: E = incident electron energy. E' = scattered electron energy for elastic scattering. E'' = energy of undetected recoil electron. k = energy of emitted photon. θ = angle of scattering observed. E' is related to θ by the kinematic relation for elastic scattering. $\Delta\theta=\theta-\theta_{\min}$. $\theta_{\min}$ = angle at slit edge representing smallest scattering angle. $\theta_{\max}$ = angle at slit edge representing largest scattering angle. m = electron rest mass. $\alpha=1/137$.

Note that in the expression for $\delta(\theta)$, the quantity $E-E'$ represents the energy carried away by the recoil electron plus the energy of the emitted photon. An integration is performed over all possible photon energies and angles, which would give electrons of the same energy and angle corresponding to elastic scattering. In this experiment electrons which radiate a photon appear to be included in the elastic electron-electron scattering peak as elastic scattering events.

The corrections as calculated for this experiment are given with the results in Sec. IV, part E. They were calculated assuming that the corrections (and cross section) are constant across the region of the peak

used for data reduction. Since the experimental results are not sensitive enough to detect such a variation, this is a good approximation.

Many assumptions were made in the derivation of $\delta(\theta)$. In order to clearly understand all of them a complete discussion of a very complicated calculation would be required. The conditions which were imposed are: (a) Throughout the calculation of $\delta(\theta)$, the rest-mass energy of the electron is neglected relative to all kinetic energies; (b) The restriction $\Delta\theta/\theta \ll 1$ must be satisfied; (c) The energy difference, $\Delta E' = E'(\theta_{\min}) - E'(\theta)$, between the two elastically scattered energies corresponding to $\theta_{\min}$ and θ in Fig. 10 must be much greater than the energy resolution of the spectrometer; (d) It is assumed that the incident electron beam is monoenergetic.

Let us now compare the experimental conditions with the restrictions (a) through (d). Since the rest-mass energy of the electron is only 0.51 Mev, condition (a) is always true. The energies involved in this experiment are all greater than 100 Mev. If one substitutes typical values for this experiment into (b), one obtains $\Delta\theta/\theta \sim 0.05$ at the 2.6 deg data point. $\Delta E' = E'(\theta_{\min}) - E'(\theta) \sim 10$ Mev, whereas the energy slits of the spectrometer were set to accept about 0.7 Mev at this point. Condition (d) is satisfied if the $\Delta E'$ in (c) is also much greater than any uncertainty of the energy of the scattered electron caused by the energy spread of the incident beam. The energy spread of the incident beam was about $\frac{1}{4}\%$, which gives an uncertainty of scattered energy of about 0.5 Mev compared to 10 Mev. An inspection of $\delta(\theta)$ shows that $\delta(\theta)$ diverges as $\Delta\theta$ approaches zero. When $\Delta\theta$ approaches zero this is equivalent to a violation of condition (c), which means $\Delta E'$ approaches zero. This behavior can be seen in the following way. The quantity $\Delta\theta/\theta$ plays approximately the role $\Delta E/E$ in the Schwinger correction, which gives an infrared divergence as E approaches zero. Thus, $\Delta\theta$ approaching zero is equivalent to an infrared divergence.

It should be mentioned why the radiative corrections do not depend on the energy resolution of the spectrometer, but instead depend on θ. In the center-of-mass system, the radiative corrections do depend on the energy resolution of a detector, but in the relativistic transformation to the laboratory system, the center-of-mass energy resolution becomes proportional to $\Delta\theta$. This statement must be qualified, since the lack of dependence on the energy resolution of the spectrometer is true only as long as the $\Delta E'$ corresponding to $\Delta\theta$ is large compared to the energy resolution of the spectrometer. This is just condition (c).

B. Comparison with Theory

The experimental results presented in part E of Sec. IV are compared to the calculation made by Tsai. The use of a χ^2 test applied to the data shows good agreement with Tsai's calculation, and the test indicates that the Møller formula should be corrected for radiative effects. However, when the data are shifted upward by the estimated 2% systematic error, the data cannot distinguish between the Møller formula and the Møller formula corrected for radiative effects.

VI. CONCLUSIONS

Although this experiment is a high resolution experiment from the experimentalist's point of view; i.e., $\Delta E'/E'$ for the scattered electron is $\sim 0.5\%$, from the point of view of radiative corrections this experiment is a low-resolution experiment. In the radiative corrections, a high-resolution experiment means that the phase space available for the emission of a photon is small and the radiative corrections are large. In this experiment, since one of the final electrons is undetected, a photon can steal almost all the energy and momentum from this electron. Therefore, the photon has a large phase space available to it in the direction of the undetected electron. Furthermore, when our experimental conditions are transformed into those in the center-of-mass system, the quantity $\Delta\theta/\theta$ in the lab system plays the role of $\Delta E/E$ in the center of mass system. In this experiment $\Delta\theta/\theta \sim 0.1$ which is not very small. Thus, our experiment is a low-resolution experiment from the point of view of radiative corrections and thus the radiative corrections are small.

In spite of the fact that the experiment is a low-resolution experiment and the smallness of the radiative corrections makes the experimental verification of their rather difficult, we can look at our result from a more constructive point of view.

Essentially, what has been verified is that the Møller formula at this energy is a good approximation and the radiative correction becomes almost negligible when the resolution is low or when the phase space available to the emission of a photon is large. Although a theoretical calculation is more complicated for low-resolution experiments than for high-resolution experiments (where multiple photon emission can be neglected), it predicts a small radiative correction for low-resolution experiments such as this one. In this sense, the experiment agrees well with the prediction of quantum electrodynamics.

In order to perform an experiment in which the radiative corrections are enhanced, one must perform a coincidence experiment with energy analysis of both particles in order to sufficiently limit the phase space of the particle which is undetected in the present experiment. In the present experiment, there is such freedom of phase space that the radiative effects are very small and difficult to measure accurately.

ACKNOWLEDGMENTS

It is a pleasure to thank the many people who made the completion of this experiment possible. In partic-

ular, I want to express my gratitude to Eddie Wright and Ed Pathway for assistance in the machine shop; Bert Chambers for design work; Gordon Gilbert and the accelerator crew and operators; Jim Absher and the electricians, and Carl Olson and the electronic technicians.

I also owe thanks to Dr. Franz Bumiller and Dr. Jerome Friedman for their help and advice, and to Dr. Y. S. Tsai for his helpful discussions concerning the calculation. The person who initiated this experiment is Professor Robert Hofstadter, and I thank him very much for his advice and support.

PHYSICAL REVIEW VOLUME 123, NUMBER 5 SEPTEMBER 1, 1961

5-Bev Neutron Cross Sections in Hydrogen and Other Elements*

JOHN H. ATKINSON,† WILMOT N. HESS,‡ VICTOR PEREZ-MENDEZ, AND ROGER WALLACE
Lawrence Radiation Laboratory, University of California, Berkeley, California

(Received April 24, 1961)

This experiment measured the neutron total and reaction cross sections at 5.0 Bev. Transmission measurements were made in good and poor geometry. The high-energy neutron beam was produced when the Bevatron circulating proton beam struck a copper target. Neutrons were identified by their production of pions in a beryllium block. The pions were then detected by a counter telescope including a gas Čerenkov counter. The threshold of this gas Čerenkov counter defined the mean effective neutron energy at 5.0±0.4 Bev, with the half-intensity points of the neutron energy distribution at 5.9 and 4.2 Bev. The cross sections measured for the various elements are (in millibarns):

	Pb	Sn	Cu	Al	C	H
σ_t	2534±105	1986±88	1158±34	614±33	319±20	33.6±1.6
σ_r	1670± 79		586±25	381±27	235±16	

The 5-Bev total cross sections are 20% below the total cross-sections measured at 1.4 Bev by Coor *et al.*, whereas the reaction cross sections remain essentially constant as a function of energy above 300 Mev. This behavior of the cross sections can be interpreted by a generalized diffraction theory developed by Glassgold and Grieder.

I. INTRODUCTION

AT 1.4 Bev the neutron total cross sections are rising with energy.[1] Williams made the prediction, based upon these data and some high-energy cosmic-ray data, that the nucleon-nucleon total cross section would be found to rise monotonically from 42 mb at 1.4 Bev to 120 mb at 30 Bev.[2] This prediction came into question with the publication of the high-energy p-p elastic scattering data of Cork, Wenzel, and Causey, which showed a decrease in the elastic scattering cross section from a peak value at 1.5 Bev.[3] In the present experiment in order to extend neutron cross sections to higher energies, the total and reaction cross sections were measured for 5-Bev neutrons in lead, copper, aluminum, and carbon to an accuracy of about 5%. The total n-p cross section was measured directly in liquid hydrogen.

The gas Čerenkov counter used in this experiment limits the effective neutron energy to a minimum of 3.5 Bev while the maximum energy available was the 6.2-Bev peak energy of the Bevatron. Knowledge of the neutron energy is critical for determining meaningful cross sections, and is quite difficult to achieve with high-energy neutron beams.

The experiment is interpreted by a new theory developed by Glassgold and Grieder to interpret high-energy scattering data.[4] This generalized diffraction theory gives expressions for the total and reaction cross sections in easily calculated closed forms that fit the neutron scattering data well from 300 Mev to 5 Bev. A simple optical model has also been fitted to our data, giving a check on our energy determination as well as the usual optical-model parameters.

II. EXPERIMENTAL METHOD

A. Experimental Arrangement

1. Beam

The neutron beam was generated by the Bevatron internal proton beam striking a $\frac{1}{2}\times\frac{1}{2}\times$3-in. copper target with the 3-in. dimension tangent to the circulating proton beam. Whenever the primary proton beam was spilled on a target, neutrons were produced in the

* This work was done under the auspices of the U. S. Atomic Energy Commission.

† Now at Ford Aeronutronic, Newport Beach, California.

‡ Now at Lawrence Radiation Laboratory, Livermore, California.

[1] T. Coor, D. A. Hill, W. F. Hornyak, L. W. Smith and G. Snow, Phys. Rev. **98**, 1369 (1955).

[2] Robert W. Williams, Phys. Rev. **98**, 1393 (1955).

[3] B. Cork, W. A. Wenzel, and C. W. Causey, Jr., Phys. Rev. **107**, 859 (1957).

[4] A. E. Glassgold and K. Greider, Phys. Rev. Letters **2**, 169 (1959).